Evidence for Asphaltene Nanoaggregation in Toluene and Heptane from Molecular Dynamics Simulations†

ARTICLE *in* ENERGY & FUELS · MARCH 2009

Impact Factor: 2.79 · DOI: 10.1021/ef800872g

3 AUTHORS:

Thomas F Headen
Imperial College London
9 PUBLICATIONS **230** CITATIONS
SEE PROFILE

Edo Boek
Imperial College London
97 PUBLICATIONS **2,198** CITATIONS
SEE PROFILE

Neal Skipper
University College London
101 PUBLICATIONS **3,802** CITATIONS
SEE PROFILE

Evidence for Asphaltene Nanoaggregation in Toluene and Heptane from Molecular Dynamics Simulations†

Thomas F. Headen,*,‡,§ Edo S. Boek,§ and Neal T. Skipper‡

Department of Physics and Astronomy, University College London, Gower Street, London WC1E 6BT, United Kingdom, and Schlumberger Cambridge Research, High Cross, Madingley Road, Cambridge CB3 0EL, United Kingdom

Received October 10, 2008. Revised Manuscript Received December 13, 2008

Molecular dynamics simulation techniques have been used to study the nanoaggregation of one resin and two asphaltene structures, generated by an updated quantitative molecular representation (QMR) technique (Boek, E. S.; Yakovlev, D. S.; Headen, T. F. *Energy Fuels*, manuscript submitted), in toluene and heptane. Analysis of the simulation trajectories, to yield the separation of asphaltene or resin pairs, over a 20 ns simulation has been used to investigate aggregation dynamics. The structure of aggregates has been investigated by the calculation of the asphaltene−asphaltene and resin−resin radial distribution functions, $g(r)$, and the average angle between the polyaromatic planes as a function of separation. We calculate, for the first time, the asphaltene−asphaltene potential of mean force (PMF) from the $g(r)$ and separately by a constraint force method. In general, it is observed that the asphaltenes form dimers and trimers in both toluene and heptane. Once formed, the dimers and trimers can separate and reform other aggregates with other asphaltene molecules. Aggregates persist for longer in heptane than in toluene. The resin molecule forms no aggregates in toluene, with some aggregation occurring in heptane. Significant peaks in the asphaltene−asphaltene $g(r)$ are seen in both toluene and heptane between 0.5 and 1 nm separation. This is strong evidence for asphaltene nanoaggregation from molecular dynamics simulations. At the lowest separations, the angle between the aromatic planes is close to parallel. The calculated potential of the mean force gives similar results for both methods. For the asphaltene molecules in both toluene and heptane, free energy of dimer formation ranged from −6.6 to −12.1 kJ mol^{-1}.

Introduction

Asphaltenes are a solubility class of crude oils and bitumens, defined as being the fraction of crude insoluble in *n*-alkanes (heptane) but soluble in aromatic solvents (toluene). This fraction has complex solubility behavior, often precipitating from the crude, leading to fouling of reservoirs and pipelines. Even when soluble in a crude or aromatic solvent, the asphaltenes are known to aggregate in the nanometer length-scale, forming "nanoaggregates".[2] There is, however, little consensus in the literature as to the size, shape, and structure of the nanoaggregates and the thermodynamic driving force behind their formation. Small-angle X-ray scattering (SAXS) and small-angle neutron scattering (SANS) provide a direct method of measuring the nanoaggregate size and shape in both deuterated aromatic solvents[3–9] and crude oils.[10–12] Shape-independent Zimm and Guinier analyses yield a nanoaggregate radius of gyration ranging from 30−100 Å, dependent upon the crude oil, asphaltene precipitation method, and the analysis method used.[4,6,8] The SAXS and SANS data can be fitted to a number of geometrical form factors, including spheres,[3–5,7] ellipsoids,[6,7] and cylinders.[4,5] However, because the polydispersity of the nanoaggregates is unknown, these results should be taken with caution. Indeed, unlike other colloidal systems, asphaltenes are a wide range of different molecules, and therefore, one shape is unlikely to be correct for the whole system. More recently, additional methods have been used to study asphaltene nanoaggregates that have given a smaller size. Investigations of asphaltenes *in situ* in oil reservoirs under equilibrium conditions gave a radius of ∼10 Å by buoyancy arguments.[13] Recent ultracentrifugation studies gave similar results, estimating a nanoaggregate diamter of 2.5 nm from the sedimentation speed of the nanoaggregates.[14] Similar sizes have also been estimated

† Presented at the 9th International Conference on Petroleum Phase Behavior and Fouling.

* To whom correspondence should be addressed. E-mail: t.headen@ucl.ac.uk.

‡ University College London.

§ Schlumberger Cambridge Research.

(1) Boek, E. S.; Yakovlev, D. S.; Headen, T. F. *Energy Fuels*, manuscript accepted.

(2) *Asphaltenes, Heavy Oils, and Petroleomics*; Mullins, O. C., Sheu, Y. E., Hammami, A., Marshall, A. G., Eds.; Springer: New York, 2007.

(3) Sheu, E. Y.; Acevedo, S. *Energy Fuels* **2001**, *15*, 702–707.

(4) Gawrys, K. L.; Blankenship, G. A.; Kilpatrick, P. K. *Langmuir* **2006**, *22*, 4487–4497.

(5) Gawrys, K. L.; Kilpatrick, P. K. *J. Colloid Interface Sci.* **2005**, *288*, 325–334.

(6) Thiyagarajan, P.; Hunt, J. E.; Winans, R. E.; Anderson, K. B.; Miller, J. T. *Energy Fuels* **1995**, *9*, 829–833.

(7) Tanaka, R.; Hunt, J. E.; Winans, R. E.; Thiyagarajan, P.; Sato, S.; Takanohashi, T. *Energy Fuels* **2003**, *17*, 127–134.

(8) Roux, J. N.; Broseta, D.; Deme, B. *Langmuir* **2001**, *17I*, 5085–5092.

(9) Sheu, E. Y. *J. Phys.: Condens. Matter* **2006**, *18*, S2485–S2498.

(10) Headen, T. F.; Boek, E. S.; Stellbrink, J.; Scheven, U. M. *Langmuir*, **2009**, *25*, 422−428.

(11) Mason, T.; Lin, M. *Phys. Rev. E: Stat., Nonlinear, Soft Matter Phys.* **2004**, *67*, 050401.

(12) Mason, T.; Lin, M. *J. Chem. Phys.* **2003**, *119*, 565–571.

(13) Mullins, O. C.; Betancourt, S. S.; Cribbs, M. E.; Dubost, F. X.; Creek, J. L.; Andrews, A. B.; Venkataramanan, L. *Energy Fuels* **2007**, *21*, 2785–2794.

(14) Mostowfi, F.; Indo, K.; Mullins, O. C.; McFarlane, R. *Energy Fuels*, **2009**, *23*, 1194-1200.

10.1021/ef800872g CCC: $40.75
Published on Web 02/02/2009

from high-Q ultrasonics.[15,16] These measurements indirectly link the asphaltene molecular structure with the colloidal structure, giving an aggregation number of 4−5. Nuclear magnetic resonance (NMR) diffusion measurements[17] and direct-current (DC) conductivity measurements[18] of asphaltene solutions have been shown to give similar results.

There is less agreement on the structure of asphaltene molecules within the asphaltene nanoaggregates. The most prevalent theory is that asphaltene nanoaggregates are formed from stacking of asphaltene aromatic cores; the stacking is terminated because of steric considerations.[19] This model is consistent with smaller nanoaggregate sizes from high-Q ultrasonics measurements,[15] which give an aggregation number of approximately ∼5, which is a reasonable number for $\pi-\pi$ stacking. However, this model seems incompatible with the nanoaggregate sizes measured by SAXS and SANS, because these sizes require a much greater aggregation number. SAXS and SANS data are generally more consistent with a more "diffuse" model for nanoaggregate structure. Gawrys et al. showed that, for a polydisperse disk form factor to fit the SANS data correctly, one had to include solvent entrainment within the nanoaggregates.[4] The SAXS and SANS data can alternatively be well-interpreted as fractal objects of fractal dimension ∼2.5, again indicating a diffuse nanoaggregate.[10,20] Sirota et al.[21,22] have attributed the SANS data to a solution behavior of asphaltenes as "dynamically varying compositional inhomogenities".

It is our aim in this study to investigate the structure of nanoaggregates and the driving force behind the asphaltene nanoaggregation using molecular simulation. Unfortunately, the length scales are too large and time scales are too long to fully study asphaltene nanoaggregation by atomistic molecular simulation. However, small-scale simulations can give information about aggregation of a small number of molecules, the structure, and the driving force behind the aggregation of dimers and trimers, which can be used as a guide for the most likely model for nanoaggregation.

In recent years, there has been an increasing effort to understand the structure of asphaltene aggregation on a molecular level using molecular simulation.[23–28] Initially, asphaltene aggregation was considered *in vacuo* by molecular mechanics methods. Murgich et al.[29] conducted molecular mechanics calculations using a large asphaltene structure (a single polyaromatic core containing 24 aromatic rings) and showed that aggregation mainly occurred by stacking of aromatic cores. Similarly, Pacheco-Sánchez et al.[23] used molecular dynamics to show that asphaltene aggregation does occur spontaneously for smaller asphaltene molecules (the archetypal Groenzin/Mullins model[30]), forming dimers, trimers, and tetramers during a short 100 ps simulation. The structure of the aggregates formed showed no overriding structure type: face−face, offset stacked, and T-shaped aggregates were observed. Simulations of asphaltene dimers with explicit solvent molecules conducted over 100 ps by Carauta et al.[25] have shown that the asphaltene dimers bind face−face at a distance of ∼3.6 Å in heptane and ∼5 Å in toluene. Furthermore, they show that the effect of an increasing temperature (from 323 to 573 K) is to decrease the distance between the asphaltene dimer. A similar temperature dependence has been observed by Zhang et al.[27] from molecular dynamics simulations of asphaltene molecules in model asphalts over 3 ns. The $g(r)$ showed nearest neighbor peaks at lower r at the highest temperatures. The nearest neighbor orientation of asphaltene aromatic cores also showed temperature dependence. Additionally, molecular simulation has been used to study the thermodynamics of asphaltene aggregation by obtaining asphaltene−asphaltene binding energies.[31,32] Ortega-Rodríguez et al. have conducted coarse-grained simulations,[31] representing each asphaltene molecule as a single point with a spherically symmetric interaction potential defined from atomistic molecular mechanics (MM) simulations *in vacuo*.[33] These atomistic MM calculations gave a high asphaltene−asphaltene binding energy of −130 kJ mol^{-1}. From this, they calculated the asphaltene−asphaltene $g(r)$ for course-grained simulations of model asphaltenes and resins, while solvent effects were simplified to a background dielectric constant. From the $g(r)$, the potential of mean force was calculated and the binding free energy was estimated to be $\sim -4kT$, considerably less than the binding energy from the MM calculation *in vacuo*. More detailed atomistic calculations have been conducted between asphaltene pairs in vacuum using the density functional theory by Alvarez-Ramirez et al..[32] They found an asphaltene−asphaltene binding energy of 50−63 kJ mol^{-1}.

For any of these simulation studies to yield meaningful results, the model asphaltene structures used must be representative of asphaltenes as a whole. Indeed, a range of different types of asphaltene molecular models have been used in asphaltene simulation, from archipelago-type structures with multiple small aromatic islands connected by aliphatic chains[31] to large island asphaltenes with a single large aromatic core.[29] Recent experimental studies using fluorescence depolarization measurements,[30] high-resolution mass spectroscopy,[34] and UV absorption and fluorescence emission[35,36] have all shown an asphaltene structure with a single aromatic core (possibly two) containing 4−10 aromatic rings. Previous studies have used "average" model structures that are consistent with experimental data.[25,37,38]

(15) Andreatta, G.; Goncalves, C. C.; Buffin, G.; Bostrom, N.; Quintella, C. M.; Arteaga-Larios, F.; Pérez, E.; Mullins, O. C. *Energy Fuels* **2005**, *19*, 1282–1289.
(16) Andreatta, G.; Bostrom, N.; Mullins, O. C. *Langmuir* **2005**, *21*, 2728–2736.
(17) Freed, D. E.; Lisitza, N. V.; Sen, P. N.; Song, Y. Q. Asphaltene molecular composition and dynamics from NMR diffusion measurements. *Asphaltenes, Heavy Oils, and Petroleomics*; Mullins, O. C., Sheu, Y. E., Hammami, A., Marshall, A. G., Eds.; Springer: New York, 2007; Chapter 11.
(18) Zeng, H.; Song, Y.; Johnson, D. L.; Mullins, O. C. *Energy Fuels*, manuscript submitted.
(19) Buenrostro-Gonzalez, E.; Groenzin, H.; Lira-Galeana, C.; Mullins, O. C. *Energy Fuels* **2001**, *15*, 972–978.
(20) Barre, L.; Simon, S.; Palermo, T. *Langmuir* **2008**, *24*, 3709–3717.
(21) Sirota, E. B. *Energy Fuels* **2005**, *19*, 1290–1296.
(22) Sirota, E. B.; Lin, M. Y. *Energy Fuels* **2007**, *21*, 2809–2815.
(23) Pacheco-Sánchez, J. H.; Zaragoza, I. P.; Martínez-Magadán, J. M. *Energy Fuels* **2003**, *17*, 1346–1355.
(24) Pacheco-Sánchez, J. H.; Álvarez-Ramírez, F.; Martínez-Magadán, J. M. *Energy Fuels* **2004**, *18*, 1676–1686.
(25) Carauta, A. N. M.; Seidl, P. R.; Chrisman, E. C. A. N.; Correia, J. C. G.; Menechini, P. O.; Silva, D. M.; Leal, K. Z.; de Menezes, S. M. C.; de Souza, W. F.; Teixeira, M. A. G. *Energy Fuels* **2005**, *19*, 1245–1251.
(26) Carauta, A. N. M.; Correia, J. C. G.; Seidl, P. R.; Silva, D. M. *J. Mol. Struct.* **2005**, *755*, 1–8.
(27) Zhang, L.; Greenfield, M. L. *Energy Fuels* **2007**, *21*, 1102–1111.
(28) Zhang, L.; Greenfield, M. L. *J. Chem. Phys.* **2007**, *127*, 194502.
(29) Murgich, J.; Rodríguez, M, J.; Aray, Y. *Energy Fuels* **1996**, *10*, 68–76.
(30) Groenzin, H.; Mullins, O. C. *Energy Fuels* **2000**, *14*, 677–684.
(31) Ortega-Rodríguez, A.; Cruz, S. A.; Gil-Villegas, A.; Guevara-Rodríguez, F.; Lira-Galeana, C. *Energy Fuels* **2003**, *17*, 1100–1108.
(32) Alvarez-Ramirez, F.; Ramirez-Jaramillo, E.; Ruiz-Morales, Y. *Energy Fuels* **2006**, *20*, 195–204.
(33) Ortega-Rodríguez, A.; Cruz, S. A.; Ruiz-Morales, Y.; Lira-Galeana, C. *Pet. Sci. Technol.* **2001**, *19*, 245.
(34) Rodgers, R. P.; Marshall, A. G. Petroleomics: Advanced characterisation of petroleum derived materials by Fourier transform ion cyclotron resonance mass spectrometry (FT-ICR MS). *Asphaltenes, Heavy Oils, and Petroleomics*; Mullins, O. C., Sheu, Y. E., Hammami, A., Marshall, A. G., Eds.; Springer: New York, 2007; Chapter 3.

Sheremata et al.[39] have developed quantitative molecular representation (QMR) as a method for generating a group of structures that best represent experimental data (mass spectrometry, NMR, and elemental analysis), rather than just being consistent with the data. It was shown that 5−6 molecules were needed to represent the experimental data well. The method is based on an algorithm that builds a very large number of asphaltene molecules from building blocks. From this set, the best mixture of 5−6 molecules are chosen that fit the experimental data. This method has recently been updated[1] to allow for the formation of smaller (one aromatic core) and three-dimensional structures. This gives the best fit to experimental data with low-molecular-weight asphaltenes (500−2000 amu). This is quite different from the asphaltene molecular weight used by Sheremata et al.,[39] where a molecular weight of ∼4000 Da, determined from VPO, was used. This tends to the conclusion that asphaltenes have just one or perhaps two aromatic cores, because larger archipelago-type models would have too high of a molecular weight.

In this paper, we report on molecular dynamics (MD) simulations of three asphaltene structures generated from a preliminary version of the updated QMR method in both toluene and heptane. From the simulations, we obtain the distance−time relationship over 20 ns between asphaltene pairs to reveal the time scale of aggregation. From this, we aim to discover whether aggregation is permanent over several nanoseconds or whether asphaltene dimers/trimers form separate and reform indicating solution behavior. We also obtain the asphaltene−asphaltene radial distribution function $g(r)$ and the average angle between the aromatic planes as a function of the distance to directly detect the structure of asphaltene aggregation in dimers and trimers; this can indicate the structure of larger asphaltene nanoaggregates. Lastly, we use the asphaltene−asphaltene $g(r)$ and force−distance data from constrained simulations of asphaltene pairs to calculate the asphaltene−asphaltene potential of mean force (PMF). This allows us to calculate an estimate for the binding free energy between asphaltene molecules, fully taking into account solvent effects.

Simulation Methods

Classical molecular dynamics uses well-defined classical intra- and intermolecular potentials to calculate interatomic forces. The system is allowed to evolve over time by stepwise integration of the equations of motion. It is important that the step size be smaller than the time period of the fastest motion in the simulation. Using this method, it is possible to simulate systems containing a total of ∼10 000 atoms over a few nanoseconds on ∼8 processor nodes in reasonable times. For this study, the GROMACS MD code[40] with the OPLS-AA force-field parameters[41,42] was used. The OPLS force field has been shown to work well for aromatic liquids in reproducing experimental data.[42] We have tested the applicability of the force field to polyaromatics by conducting NPT simulations on bulk 1-methylnaphthalene. The values obtained for density and enthalpy of vaporization are close to experimentally determined values.[43] Results are given in Table 1.

Table 1. Comparison of Enthalpy of Vaporization and Density of 1-Methylnaphthalene Obtained from MD Simulation Using OPLS-AA Force Field with Experimentally Determined Values[43]

	experiment	NPT simulation
enthalpy of vaporization (kJ mol^{-1})	57.5	59.4
liquid density (g cm^{-3})	1.001	1.020

Rigid bond lengths were used to remove the fastest moving molecular motions. Bond angles and dihedral angles remained flexible (within appropriate force fields) to allow for molecular flexibility. A time step of 2 fs was used for all simulations. This was decided upon after conducting NVE simulations of toluene with time steps of 1, 2, 5, and 10 fs. Simulations with time steps of 5 or 10 fs showed some energy loss during the simulation. Periodic boundary conditions with the minimum image convention are used, so that a small box of ∼10 000 atoms can represent the bulk. Long-range coulomb intermolecular forces are treated using the particle-mesh Ewald (PME) technique,[44] which allows for the use of fast-Fourier transforms (FFT).

In this study, two types of simulations were conducted:

(i) A simulation of six asphaltene molecules in toluene or heptane at 7 wt % over 20 ns. A concentration of 7 wt % is similar to the asphaltene concentration of many crude oils and allows the study of six asphaltene molecules in a suitably sized simulation cell. Analysis of the trajectory of the full NVT simulation allows for the calculation of the asphaltene−asphaltene radial distribution function, $g(r)$. The $g(r)$ is defined as a ratio of the local density of atoms/molecules at a distance r from an atom at the origin to the average density of atoms in the bulk

$$g(r) = \frac{\rho(r)}{\rho} \tag{1}$$

In this case, r is the distance between a single atom defined on each asphaltene molecule to represent its center. The cumulative coordination number can be calculated from the $g(r)$ by integration over spherical shells thickness dr.

$$N(r) = \int_0^r \rho g(r) 4\pi r^2 \mathrm{d}r \tag{2}$$

In essence, this is the number of other asphaltene molecules within the sphere radius r centered on the original molecules. Another useful quantity that may be calculated from the $g(r)$ is the potential of mean force (PMF). In the low-density limit, the pair potential is given by[45]

$$u(r) = -kT \ln(g(r)) \tag{3}$$

This concept can be extended to dense fluids by defining the potential of mean force as

$$W = -kT \ln(g(r)) \tag{4}$$

The PMF is equivalent to the Helmholtz free energy (plus a constant). We can therefore calculate the free energy of dimer formation by taking the difference of the potential of mean force at maximum separation and at equilibrium separation (where the PMF is a minimum).

(ii) Calculating the potential of mean force by a constraint force method: A series of simulations of pairs of asphaltene molecules in toluene or heptane is conducted in which the distance between the center of mass of the two asphaltenes is constrained using the

(35) Ruiz-Morales, Y.; Wu, X.; Mullins, O. C. *Energy Fuels* **2007**, *21*, 944–952.
(36) Ruiz-Morales, Y.; Mullins, O. C. *Energy Fuels* **2007**, *21*, 256–265.
(37) Groenzin, H.; Mullins, O. C. *Energy Fuels* **2000**, *14*, 677–684.
(38) Murgich, J.; Rodríguez, J. M.; Aray, Y. *Energy Fuels* **1996**, *10*, 68–76.
(39) Sheremata, J. M.; Gray, M. R.; Dettman, H. D.; McCaffrey, W. C. *Energy Fuels* **2004**, *18*, 1377–1384.
(40) van der Spoel, D.; Lindahl, E.; Hess, B.; Groenhof, G.; Mark, A. E.; Berendsen, H. J. C. *J. Comput. Chem.* **2005**, *26*, 1701–1718.
(41) Jorgensen, W. L.; Maxwell, D. S.; Tirado-Rives, J. *J. Am. Chem. Soc.* **1996**, *118*, 11225–11236.
(42) Jorgensen, W. L.; Laird, E. R.; Nguyen, T. B.; Tirado-Rive, J. *J. Comput. Chem.* **1993**, *14*, 206–215.
(43) Sabbah, R.; Chastel, R.; Laffitte, M. *Thermochim. Acta* **1974**, *10*, 353–358.
(44) Darden, T.; York, D.; Pedersen, L. *J. Chem. Phys.* **1993**, *98*, 10089–10092.
(45) Lee, L. L. *Molecular Thermodynamics of Nonideal Fluids*; Butterworths: Boston, MA, 1988.

SHAKE algorithm.[46] The constraint distances used were from 0.3 to 1.5 nm, in steps of 0.1 nm. At each time step during the simulation, the force required to keep the molecules at the constraint distance is calculated by the SHAKE algorithm. This is averaged over the 20 ns simulation to give a mean force between the molecules over millions of molecular conformations. Integration of the force−distance curve yields the PMF (plus a constant of integration). This therefore provides an alternative method of calculating the PMF and the free energy of asphaltene aggregation. It is more computationally expensive than calculation of the PMF from the $g(r)$; however, it does have the advantage that it samples more of the ensemble in high-energy configurations, such as when the asphaltenes are held very close together. It can therefore provide a more accurate estimate for the PMF at distances that are not well-sampled during an unconstrained simulation. The PMF calculated by this method also includes an entropic contribution because of the decrease in entropy as one reduces the distance between the molecules. This is essentially the PMF of two non-interacting masses constrained to be at a distance r apart, given by[47]

$$V_0 = -2kT \ln(r) \quad (5)$$

Therefore, this entropic contribution must be subtracted for comparison to the PMFs calculated from the $g(r)$ using eq 4.

For simulations of type i, the simulation system was created by periodically arranging the asphaltene molecules in a box of appropriate size (dependent upon how many solvent molecules needed to be added to make 7 wt % asphaltene). A periodic arrangement of solvent molecules was then added, with any molecules overlapping the asphaltene molecules being removed. For simulations of type ii, the asphaltenes are arranged in a box of size 5 × 5 × 5 nm, with the centers of mass the appropriate distance apart. The asphaltenes are arranged with the aromatic cores parallel to each other and solvent molecules added using the method as above. For both simulation types, the system was equilibrated initially by a 100 ps NVT simulation, followed by a 500 ps NPT simulation for the system to reach equilibrium density. Sampling was conducted during the main 20 ns NVT simulation. Temperature was maintained at 300 K using the Nose−Hoover thermostat, and the Parrinello−Rahman barostat was used for the NPT equilibration.

The asphaltene structures used were generated using a preliminary version of the modified QMR method of Boek et al.[1] The basis of the method is to generate a group of ∼10 000 asphaltene structures that make chemical sense. An algorithm is then used to select a mixture of 5−6 structures and their proportions in the mixture that give the best match to the available experimental data (^{1}H and ^{13}C NMR and elemental analysis) for a particular asphaltene. The average molecular weight was chosen to be 750 Da; this molecular weight gave the lowest value of the objective function in the QMR method and agrees well with recent values for asphaltene molecular weight proposed in the literature by high-resolution mass spectroscopy.[24] The set of asphaltenes chosen for this study had five asphaltene molecules, two of which were below 5% in the mixture. Therefore, only the remaining three were studied because they represented the majority of asphaltenes in the mixture. A further reason for choosing this set of structures is that it covers a range of molecular types. One molecule has a small aromatic core (two aromatic rings) and a low molecular weight and is therefore more like a resin than an asphaltene. For this reason, this molecule shall be referred to as "resin B" throughout the paper (Figure 2). Asphaltene A represents an archipelago-type asphaltene model with two aromatic cores (Figure 1). Of the three structures studied, asphaltene C is the asphaltene with its structure best matched to result from experimental and theoretical studies of asphaltene UV fluorescence emission and absorption spectra,[35,36] showing average aromatic core sizes of approximately seven rings. Therefore, this structure is considered in more detail than other structures. Note that these asphaltene structures were generated using a preliminary version of the QMR software described in ref 1 and should only be considered as examples of the variety of structures that can be generated and not as optimized structures. Asphaltenes A and C in Figures 1 and 3 have a relatively high deviation from the objective function and, as such, are not the best molecular representations of the experimental data. They are presented here only to consider the archipelago and island structure hypothesis. For a set of more accurate structures, see ref 1.

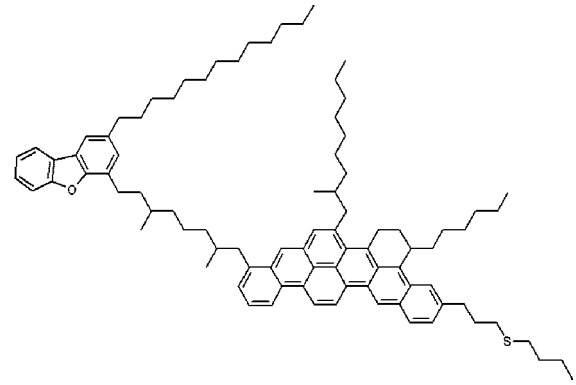

Figure 1. Chemical structure of asphaltene A. An "archipelago"-type asphaltene with two condensed aromatic cores connected by an aliphatic chain.

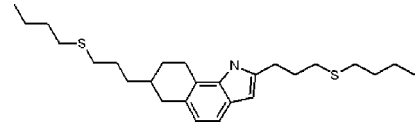

Figure 2. Chemical structure of resin B. A structure at the resin end of the asphaltene spectrum.

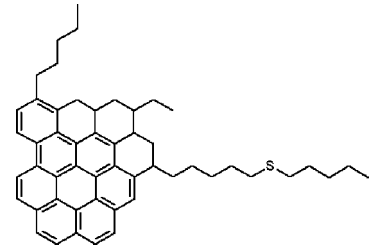

Figure 3. Chemical structure of asphaltene C. An "island"-type asphaltene structure with one large pericondensed aromatic core.

Results and Discussion

Distance between Asphaltene Molecules during Unconstrained MD Simulations of Asphaltenes at 7 wt %. Over the course of the simulation, the atomic positions are recorded every 4 ps. From this, the distance between the center of mass (com) of asphaltene molecules over the course of the simulation can be obtained. Figures 4 and 5 show the distance between the asphaltene pairs showing aggregation during the 20 ns simulation, in toluene and heptane, respectively. The distance−time curves for other asphaltene pairs, showing no aggregation, have been left out for clarity. For all distance−time plots, a running average of every 500 ps is taken to reduce the scatter in the data.

Both plots show a distinct and stable dimer state, with the distance between the aromatic cores below 1 nm. The simulation in toluene shows that dimers and trimers form, separate, and reform with different molecules; there is no lasting aggregation. Trimers can be located by finding two aggregated "pairs" with

(46) Ryckaert, J. P.; Ciccotti, G.; Berendsen, H. J. C. *J. Comput. Phys.* **1997**, *23*, 327–341.

(47) van der Spoel, D.; Lindahl, E.; Hess, B.; van Buuren, A. R.; Apol, E.; Meulenhoff, P. J.; Tieleman, D. P.; Sijbers, A. L. T. M.; Feenstra, K. A.; van Drunen, R.; Berendsen, H. J. C. Gromacs User Manual, version 3.3, 2005; www.gromacs.org.

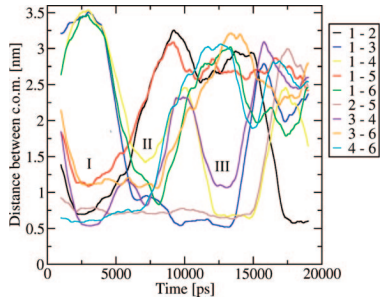

Figure 4. Distance between centers of mass of six molecules of asphaltene C in toluene over 20 ns MD simulation for all asphaltene pairs that show aggregation. There is a well-defined aggregated state for com−com distances below ∼1 nm. Dimers and trimers are short-lived, forming, breaking-up, and reforming over the course of the simulation.

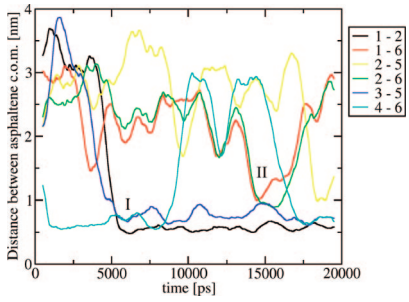

Figure 5. Distance between centers of mass of six molecules of asphaltene C at 300 K in heptane over 20 ns MD simulation for all asphaltene pairs that show aggregation. Two of the dimers that are formed remain aggregated for the rest of the simulation, indicating longer lasting aggregation in heptane than seen in toluene.

a common asphaltene. At point I in Figure 4, at approximately 3 ns, the distance−time curves reveal that a pair of trimers had been formed in solution between asphaltenes 1, 2, and 5 and 3, 4, and 6. It is clear that the distances between the pairs are not equal in the trimer, signifying that there is one central asphaltene (in this case, asphaltenes 2 and 4) "sandwiched" between two other asphaltenes, most likely in a stacked arrangement. Figure 6 is a snapshot of the simulation at point I, showing the formation of two stacked trimers. Interestingly, *loose* rather than *rigid* stacking of the aromatic cores is observed; i.e., the aggregate lasts for only a few nanoseconds, and even during this time, its conformation is constantly changing. There is no single, minimum energy, aggregated structure. This can be observed clearly in Figure 4. In going from time I to time II (at approximately 7 ns), asphaltene 1 separates from its trimer with asphaltenes 2 and 5 to form a new trimer with asphaltenes 3 and 6. Approximately 6 ns later at point III, asphaltene 6 breaks from the trimer and is replaced by asphaltene 4. Asphaltenes 2 and 5 are the longest aggregated pair, staying in the aggregated state for approximately 15 ns. It is important to note that the formation of asphaltene clusters, mainly as dimers and trimers, is also seen in solid precipitated asphaltenes studies using high-resolution transmission electron microscopy (HRTEM).[48]

In heptane, more permanent dimer formation is observed.. For two asphaltene pairs (asphaltenes 1−2 and 3−5), there is no separation once aggregation has occurred. Figure 7 shows a snapshot of the simulation in heptane at point I (∼6 ns), in which three dimers are observed. This snapshot shows clearly that although stacking of the aromatic cores is a preferred aggregation geometry, the stacking is not exclusively parallel $\pi-\pi$-

(48) Sharma, A.; Groenzin, H.; Tomita, A.; Mullins, O. C. *Energy Fuels* **2002**, *16*, 490.

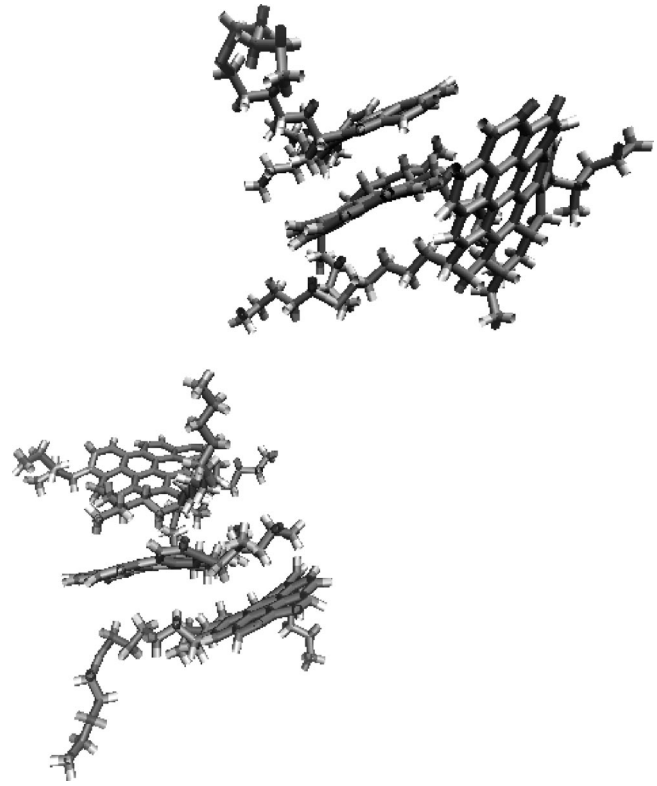

Figure 6. Snapshot of MD simulation of six molecules of asphaltene C in toluene at 300 K at point I (at ∼3 ns) showing the formation of two trimers. Toluene molecules have been removed for clarity. Parallel and nonparallel stacking of aromatic cores is observed.

stacked. The lower dimers in the snapshot show close contact between the aromatic cores and the aliphatic chains of the molecules. Trimer formation is also observed in heptane at time II (∼14.5 ns).

The simulations with asphaltene C were repeated at the higher temperature of 350 K to investigate how increasing the temperature may change the aggregation dynamics. The distance−time curves are qualitatively similar to those from simulations conducted at 300 K. We therefore define an average aggregation time to attempt to quantify the differences between asphaltene aggregation in the system. We define a critical aggregation distance, below which asphaltene pairs are considered to be aggregated, and a critical aggregation time, above which an asphaltene pair is considered to be aggregated. The values used were 1 nm for the critical aggregation distance, because just below 1 nm, a clear aggregated state is visible in the distance−time plots, and 500 ps for the critical aggregation time. These values are somewhat arbitrary; however, they are useful to allow for a comparison of the simulations. We then count the length of each aggregation event and find the mean aggregation time. Table 2 gives the mean aggregation time and number of aggregation events (in parentheses) for resin B and asphaltene C in toluene and heptane.

There is a marked decrease in the average aggregation time with temperature, approximately halving in both toluene and heptane with an increase of 50 K. As expected, the aggregation times are longer in heptane than in toluene. This effect is most noticeable for resin B, having considerably more and longer aggregation events in heptane than in toluene. The aggregation times for asphaltene C in heptane are probably an underestimate because, from the distance−time plots, it is clear that the aggregates are stable almost as long as the simulation itself. Therefore, longer simulations are required to obtain a more accurate value. Resin B has considerably lower aggregation

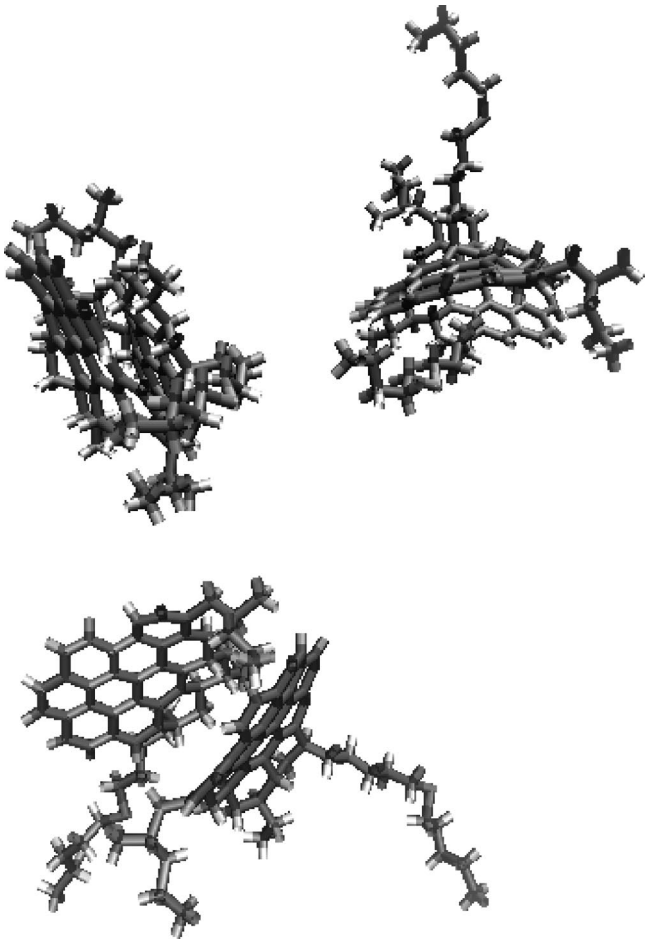

Figure 7. Snapshot of MD simulation of six molecules of asphaltene C in heptane at point I (at ~7 ns) showing the formation of three dimers. Heptane molecules have been removed for clarity. The lower dimer in the snapshot shows close contact between the aromatic cores and the aliphatic chains of the molecules.

Table 2. Average Aggregation Times during 20 ns Simulations of Six Asphaltene and Resin Molecules in Toluene and Heptane at 7 wt %

average aggregation time (in ps) (number of aggregation events)	heptane	toluene
resin B, 300 K	1623 ± 153 (67)	993 ± 104 (17)
asphaltene C, 300 K	2420 ± 473 (15)	1751 ± 243 (22)
asphaltene C, 350 K	1282 ± 157 (19)	886 ± 73 (16)

times than asphaltene C at 300 K. Figure 8 shows the distance between the pairs of resin B molecules over the 20 ns simulation in toluene. Only pairs with one resin molecule are shown for clarity; all other pairs show similar behavior. Unlike the simulations with asphaltene C, there is no well-defined aggregated state; dimer formation appears short-lived, again indicating that there is no tendency for molecular aggregation. This is to be expected because experimental studies, SAXS,[49] and Ultrasonics[15] have shown that the nanoaggregation that occurs for asphaltenes does not occur for the resins.

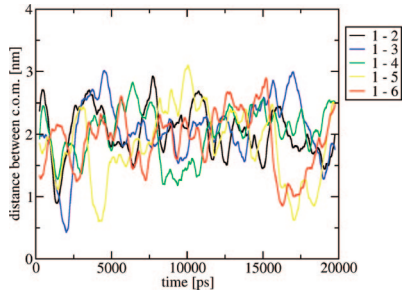

Figure 8. Distance between centers of mass of six molecules of one molecule of resin B with five others for MD simulation in toluene over 20 ns. Unlike simulations of asphaltene C, there is no well-defined "aggregated" state.

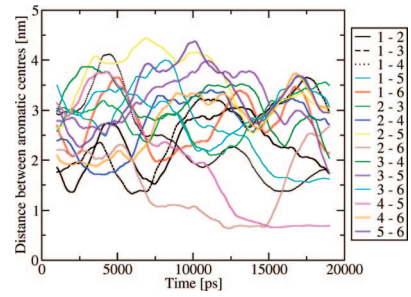

Figure 9. Distance between centers of aromatic cores for molecules of asphaltene A in toluene over 20 ns MD simulation.

Asphaltene A is an "archipelago"-type asphaltene, with two aromatic cores connected by an aliphatic chain. It therefore has no well-defined center, and being larger, its diffusion is much slower. Figure 9 shows the distance between the *center of the large aromatic cores* over the course of simulation in toluene (a similar distance−time behavior is observed in heptane). In this case, it is difficult to define an "aggregated state" between a pair of archipelago asphaltene molecules by just considering the distance between the largest aromatic cores. The reason is that, for such a large molecule, some aggregation is possible without a close approach of the aromatic cores, as shown in a snapshot of the simulation (Figure 10).

Asphaltene−Asphaltene $g(r)$ from Unconstrained MD Simulations of Asphaltenes at 7 wt %. Figure 11 shows the asphaltene C−asphaltene C $g(r)$ calculated from the asphaltene center of mass in toluene and heptane at 300 and 350 K. Two clear peaks are seen at 0.75 and 0.83 nm. There is little difference between the $g(r)$ from simulations in toluene and heptane. This result is initially surprising. However, aggregation of asphaltenes does occur in toluene, but it is terminated at the nanoaggregate length scale. For this simulation, there is a small difference in the heights of the two peaks between the solvents, with heptane having the greater $g(r)$ at 7.5 nm and toluene having the greater $g(r)$ at 0.82 nm. The peak distances are considerably greater than the $\pi-\pi$ stacking distance seen in solid asphaltenes of ~3.5 Å, indicating that a T-stacked or offset stacked aggregation geometry is preferred. A repeat simulation, with different initial molecule positions and velocities, was performed at 300 K to check the reproducibility of the $g(r)$, shown in Figure 12. The $g(r)$ values are reproducible, with only slight changes in peak height. In the second simulation, there is no difference between the behavior in toluene and heptane. Therefore, we must conclude that, at the length scale studied, the aggregation behavior of asphaltene C in toluene and heptane is very similar.

The cumulative coordination number, calculated using eq 2, is shown as dashed lines in Figure 11. The $N(r)$ illustrates that, although there are clear peaks in the $g(r)$, the actual number of molecules at these peaks is small. At ~0.75 nm, the position of the first peak in the $g(r)$, the $N(r)$ is ~0.45 molecules. The average number of neighboring molecules reaches 1 at a distance

(49) Sheu, E. Y. Pertoleomics and characterisation of asphaltene aggregates using small angle scattering. *Asphaltenes, Heavy Oils, and Petroleomics*; Mullins, O. C., Sheu, Y. E., Hammami, A., Marshall, A. G., Eds.; Springer: New York, 2007; pp 353−374.

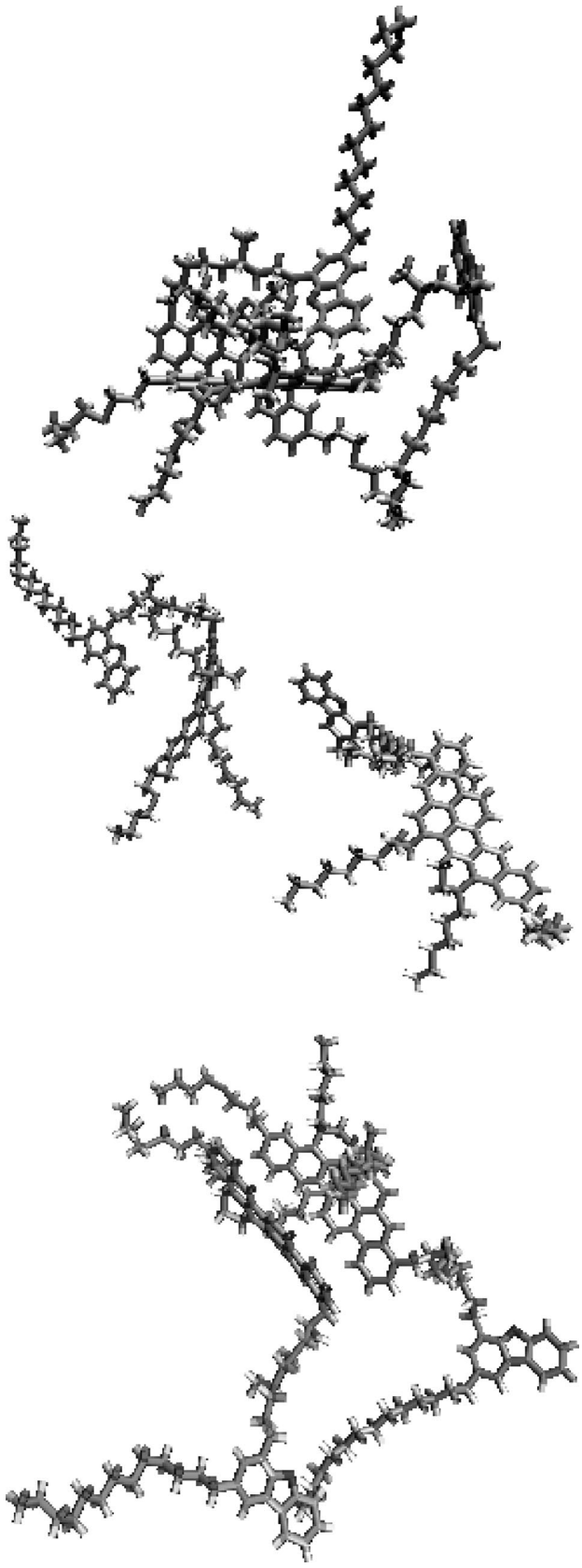

Figure 10. Snapshot of MD simulation of six molecules of asphaltene A in toluene. Aggregated conformations of molecules are considerably more complex than with asphaltenes B or C because of asphaltene being "archipelago" type.

of ~1.25 nm. Increasing the temperature decreases the $g(r)$ peak heights in both toluene and heptane; i.e., there is a slight decrease in asphaltene aggregation with an increasing temperature.

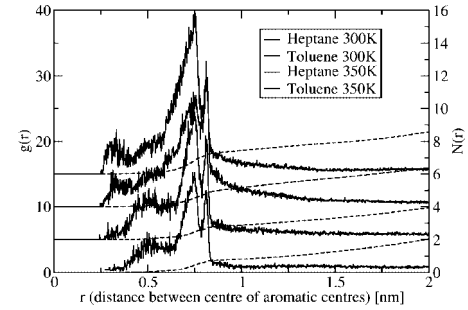

Figure 11. Asphaltene C−asphaltene C $g(r)$ and $N(r)$ for 20 ns simulations of 7 wt % asphaltene in toluene. For clarity, $g(r)$ values are offset by 5. From the top, $g(r)$ and $N(r)$ values are for simulations in heptane at 300 K, toluene at 300 K, heptane at 350 K, and toluene at 350 K. The $g(r)$ values are similar in toluene in heptane, indicating same nanoaggregation behavior. Two clear peaks in $g(r)$ are observed at 0.75 and 0.83 nm.

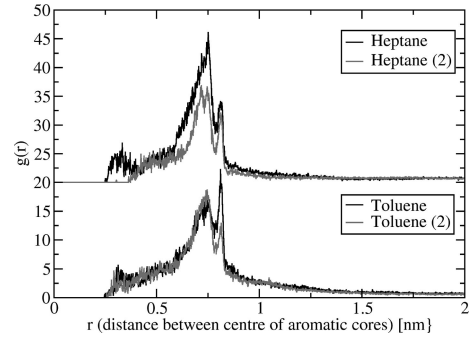

Figure 12. Asphaltene C−asphaltene C $g(r)$ from two separate 20 ns simulations in toluene and heptane. The shape of $g(r)$ is reproducible with only a slight change in peak heights observed. Very little difference between the behavior in toluene and heptane is observed.

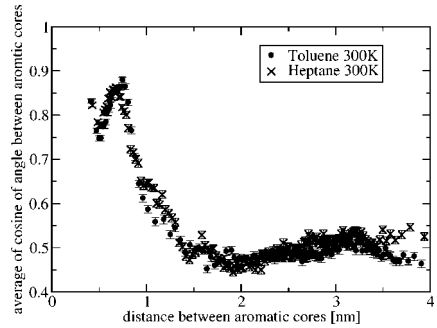

Figure 13. Average of the cosine of the angle between the aromatic planes of molecules of asphaltene C as function of the distance between asphaltene centers of mass for simulations in toluene (●) and heptane (×). In both toluene and heptane, the average cosine is close to 1 at the smallest distances, indicating parallel stacking.

Similar behavior with temperature has been observed in SANS experiments of asphaltenes in toluene[8] and crude oil.[10]

Figure 13 shows the *average* cosine of the angle between the aromatic planes as a function of the distance. At ~7.5 Å, which corresponds to the largest peak in the $g(r)$, the angle between the aromatic planes has a minimum with $\cos\theta \approx 0.85$. This indicates that an offset stacked arrangement of aggregated asphaltene molecules is the most favorable nearest neighbor interaction.

Figure 14 shows the resin−resin $g(r)$ and $N(r)$ for 7 wt % simulation of resin B in toluene and heptane. For resin B, there is a large difference in the $g(r)$ between toluene and heptane. In heptane, there is a large peak at ~0.5 nm, an indication of aggregation. In toluene, there is only a very small asphaltene−asphaltene correlation, this is also evident from the larger value

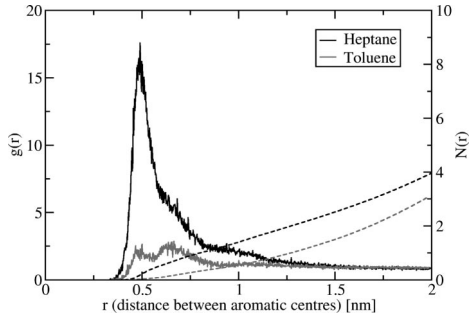

Figure 14. Resin B−resin B $g(r)$ and $N(r)$ for 20 ns simulations of 7 wt % asphaltene in toluene (gray) and heptane (black). $N(r)$ values are the dashed curves. In toluene, almost no aggregation is observed. In heptane, there is a large peak at ∼0.5 nm, indicating strong aggregation.

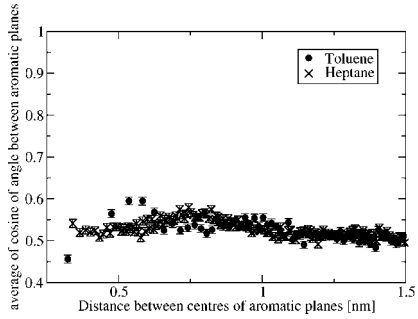

Figure 15. Average of the cosine of the angle between the aromatic planes of molecules of resin B as function of the distance between the center of the aromatic cores for simulations in toluene (●) and heptane (×). The average cosine is 0.5 at all distances, indicating that asphaltenes are randomly oriented around each other.

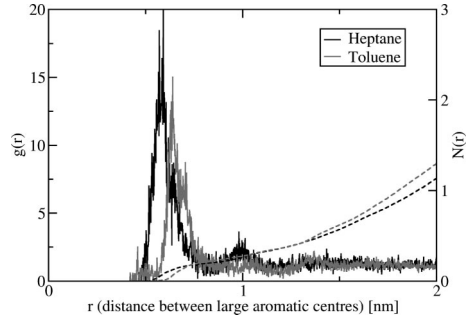

Figure 16. Asphaltene A−asphaltene A $g(r)$ (—) and $N(r)$ (- - -) for 20 ns simulations of 7 wt % asphaltene in toluene (gray) and heptane (black). The initial peak is larger and at smaller r than in toluene, signifying a stronger aggregation in heptane.

of $N(r)$ in heptane. The average angle between the aromatic planes in both toluene and heptane shows no variation with distance (Figure 15). This is perhaps unsurprising because resin B has a small polyaromatic core (only two aromatic rings). The small aromatic core means that there is only a limited $\pi-\pi$ interaction, which is not strong enough to compete with the loss of conformational entropy when asphaltenes are kept to a parallel arrangement.

Figure 16 shows the asphaltene A $g(r)$ and $N(r)$ for the center of the largest aromatic core in toluene and heptane. Large peaks are seen in both toluene and heptane, indicating aggregation of the aromatic centers. In toluene, the peak is lower and shifted to longer distances (0.66 nm) than in heptane (0.6 nm), signifying an increased aggregation in heptane compared to toluene. Interestingly, there is also a difference in the distance−angle plot for the aromatic core between toluene and heptane (Figure 17). In heptane, a parallel stacked arrangement

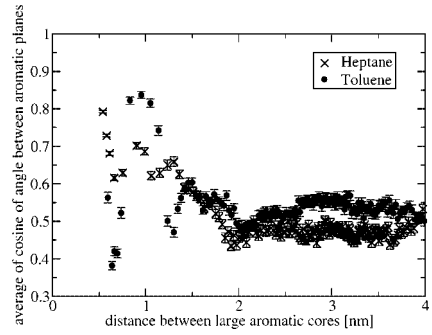

Figure 17. Average of the cosine of the angle between the aromatic planes of molecules of asphaltene A as function of the distance between the center of the aromatic cores for simulations in toluene (●) and heptane (×). In heptane, the most parallel arrangement of aromatic cores is seen at the minimum distance (∼0.5 nm). In toluene at the minimum distance, the average cosine is 0.5, indicating random arrangement. Near parallel arrangement is seen at ∼1 nm separation.

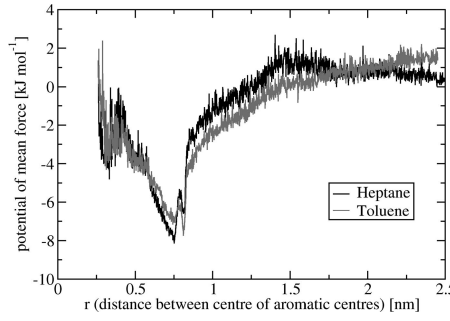

Figure 18. Potential of mean force for asphaltene C pairs from $g(r)$. From simulation of 7 wt % asphaltene C in toluene (gray) and heptane (black) at 300 K.

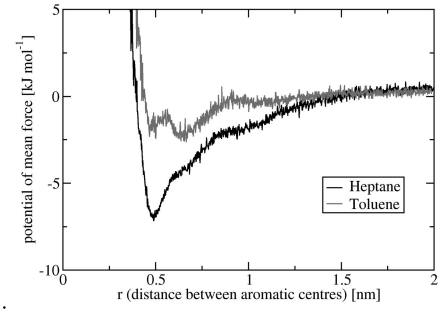

Figure 19. Potential of mean force for resin B pairs from $g(r)$. From simulation of 7 wt % asphaltene B in toluene (gray) and heptane (black) at 300 K.

of the aromatic cores is preferred at the smallest distances (∼0.5 nm), whereas in toluene, the stacking occurs at longer distances between the aromatic cores (∼1 nm). In general, these $g(r)$ values and distance−angle curves show that nanoaggregation occurs in both toluene and heptane, chiefly because of off-set stacking of the polyaromatic core. The time−separation curves show that aggregation between specific individual molecules is not long lasting and that, in this case, aggregation is limited to dimers or trimers. It is important to note, however, that firm conclusions on the aggregation number of nanoaggregates are not possible because of the small size of the system simulated.

From the asphaltene−asphaltene (or resin−resin) $g(r)$, the PMF between asphaltene or resin pairs can be estimated using eq 4. Figures 18−20 give the asphaltene−asphaltene (or resin−resin) PMF in toluene and heptane.

The free energy of dimer formation can be considered to be the potential difference between the potential at the maximum

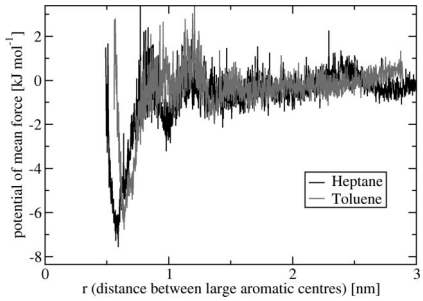

Figure 20. Potential of mean force for asphaltene A pairs from $g(r)$. From simulation of 7 wt % asphaltene A in toluene (gray) and heptane (black) at 300 K.

Table 3. Free Energy of Asphaltene/Resin Dimer Formation for Asphaltenes in Toluene and Heptane Estimated from the Potential of Mean Force Calculated from Asphaltene−Asphaltene $g(r)$

	toluene (kJ mol^{-1})	heptane (kJ mol^{-1})
asphaltene A, 300 K	–6.6 ± 1.2	–7.5 ± 1.0
resin B, 300 K	–2.4 ± 0.7	–7.3 ± 0.4
asphaltene C, 300 K	–9.0 ± 0.6	–8.2 ± 0.7
asphaltene C, 350 K	–9.0 ± 0.7	–8.4 ± 0.8

distance and the minimum potential. Table 3 gives the free energy of dimer formation for each of the asphaltenes in toluene and heptane. Only resin B shows a large difference between the toluene and heptane. For the asphaltene molecules, values of free energy of dimer formation are very similar in both toluene and heptane, varying from −6.6 to −9 kJ mol^{-1}. This is a relatively small value at around $3kT$, indicating generally weak aggregation between asphaltene molecules. It is safe to assume that further aggregation, e.g., adding an another asphaltene molecule to a dimer to form a trimer, would result in an even smaller free energy because of the increased steric interference of alkyl side chains. This explains the observation that trimers are generally short-lived in the simulations. For asphaltene C, there is little change on the free energy with temperature.

Potential of Mean Force Calculation from Constrained Pairs of Asphaltene Molecules. This method provides an alternative method for finding an estimate of the potential of mean force between pairs of asphaltene molecules that have the advantages of fully sampling the higher energy conformations at shorter distances. Figures 21 and 22 show the constraint force required to keep the distance, r, between the centers of mass of the two molecules constant for asphaltene C and resin B, respectively. Attractive forces are positive, and repulsive forces are negative. The integral of this force−distance curve

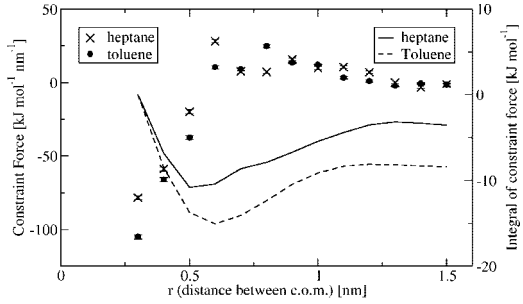

Figure 21. Constraint force and the integral of the constraint force between two molecules of asphaltene C as a function of the constraint distance for simulations in toluene (force, ●; potential, - - -) and heptane (force: ×; potential: —). Positive force is attractive, and negative force is repulsive. Similar aggregation behavior is seen in both toluene and heptane.

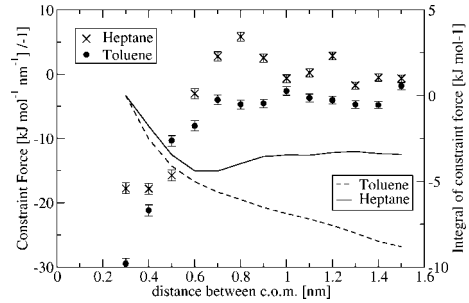

Figure 22. Constraint force and the integral of the constraint force between two molecules of resin B as a function of the constraint distance for simulations in toluene (force, ●; potential, - - -) and heptane (force, ×; potential, —). Positive force is attractive, and negative force is repulsive. No attractive force is observed in toluene, and only a small attractive force is seen in heptane.

Table 4. Free Energy of Asphaltene Dimer Formation for Asphaltenes in Toluene and Heptane Estimated from the Potential of Mean Force Calculated from the Integral of the Force−Distance Curve with Entropic Contribution (Eq 5) Subtracted

	toluene (kJ mol^{-1})	heptane (kJ mol^{-1})
resin B	n/a	–4.5 ± 2.0
asphaltene C	–12.1 ± 2.9	–11.9 ± 3.1

can be used to give an estimate of the free energy of aggregation by taking the difference between the minimum energy and the energy at large separation of molecules. To obtain a free energy of dimer formation that is consistent with the values obtained from the $g(r)$, the entropic contribution (as described by eq 5) has been subtracted from this difference. The entropic correction reduces (makes more negative) the free energy of dimer formation by ∼5 kJ mol^{-1}, depending upon the position of equilibrium separation.

Asphaltene A is a larger and more complicated molecule because it has two aromatic cores. It has therefore proven difficult to obtain satisfactory statistics in a reasonable time scale. There is also the additional difficultly that this method for obtaining the PMF is from com to com. For asphaltene A, the position of the com will vary considerably because of the archipelago structure. Table 4 gives the values for the free energy of asphaltene dimer formation calculated by this method for resin B and asphaltene C, with the entropic contribution subtracted (eq 5).

Resin B shows no attractive interaction in toluene and only a very small interaction in heptane. This is in contrast to the PMF calculated from the $g(r)$, which indeed predicts very limited aggregation in toluene but gives a larger value for the free energy in heptane. Asphaltene C shows similar free energy of dimer formation in toluene and heptane. The free energy of dimer formation calculated by this method is consistently higher (more negative) than calculated from the $g(r)$. A possible explaination for this is the fact that the concentration of asphaltenes is higher in the 7 wt % simulations; therefore, on average, the surrounding medium is more "asphaltene-like" than in the constraint force method. Interestingly, the force−distance curves for asphaltene C contain an attractive force spike at 0.6 nm in heptane and 0.8 nm in toluene; this is analogous to the two peaks seen in the $g(r)$ (Figure 11).

Conclusions

Molecular dynamics simulations of three different QMR-generated asphaltene/resin structures in baths of explicit solvent molecules (toluene and heptane) have been conducted. From

these, the separation distance−time curves have revealed the dynamics of asphaltene and resin nanoaggregation. The structure of asphaltene and resin nanoaggregates has been analyzed through calculation of the $g(r)$ and the average angle between the aromatic planes as a function of separation. Finally, the asphaltene−asphaltene and resin−resin binding energy has been calculated from the potential of mean force calculated from the $g(r)$ and a constraint force method.

The first important result to note is that asphaltene nanoaggregation occurs in both toluene and heptane, with relatively similar binding free energies, for the first time giving direct evidence linking asphaltene molecular structure to asphaltene colloidal structure. Simulations in toluene show that the formation of dimers/trimers is relatively short-lived, usually a few nanoseconds. Dimers and trimers form, break up, and form dimers/trimers with other molecules. The nanosecond lifetime may seem surprising, especially with regards to recent ultracentrifugation studies of asphaltene nanoaggregates.[14] However, this lifetime is not of asphaltene nanoaggregates but dimer formation. Nanoaggregates may well survive longer than nanoseconds, with individual asphaltene molecules diffusing in and out on a nanosecond time scale.

No larger aggregates than trimers were observed; this is most likely due to the small size of the system, only six asphaltene molecules. For simulations in heptane, the dimers/trimers are longer lived, up to the length of the 20 ns simulation. The average aggregation time decreases by approximately half on a 50 K increase in temperature. Simulations of resins in toluene and heptane show that that there is no lasting aggregation and no stable resin dimer formation is observed.

The structure of asphaltene dimers and trimers in the simulations has been analyzed by examination of the asphaltene−asphaltene radial distribution function [$g(r)$] and the average angle between the aromatic planes as a function of asphaltene separation. For the asphaltenes structures studied, this showed that a near parallel arrangement of the aromatic cores was most prevalent at the peaks in the $g(r)$ at distances between 0.5 and 1.0 nm. This suggests offset stacking as the most prevalent aggregated conformation. Observation of the simulation trajectories agrees with this. We observe that parallel asphaltene stacks do form, but they are not rigid, because the aggregated asphaltenes constantly change conformation around each other.

Asphaltene−asphaltene and resin−resin potentials of mean force calculated from the $g(r)$ and a constraint force method show similar results. The results show a relatively small free energy of asphaltene dimer formation, from ~ -3 to $-4.5kT$, with a slightly more negative free energy in heptane than toluene for the largest asphaltene (asphaltene A). This corresponds well to the asphaltene binding energy calculated by Ortega-Rodríguez et al.[31] from PMFs obtained from coarse-grained simulations of asphaltenes of $\sim 4kT$. The observation of relatively small aggregation times and low values for the free energy of dimer formation are strong evidence against the formation of *dense* nanoaggregates (no solvent entrainment or fractal nature) of the size seen by SAXS and SANS (∼5−10 nm). Forming other firm conclusions on the size of nanoaggregates from this study is impossible because of the limited size of the system studied. We cautiously suggest that a combination of specific interactions, such as the $\pi-\pi$ offset stacking seen from the simulations, and solution behavior, accounting for the larger nanoaggregate sizes seen by SAXS and SANS, would be the most reasonable model for asphaltene nanoaggregation.

These trends, however, have been deduced from just the two asphaltene structures studied here. Please note that the structures studied here should only be considered as examples and not as structures optimized for the experimental data set. Nonetheless, we believe that the main result of this paper that nanoaggregation occurs in both toluene and heptane is general and should also hold for optimized structures. A more extensive study, with a highly optimized set of QMR-generated asphaltene structures, using the simulation and analysis techniques outlined in this paper, is required if we are to confirm this conclusion. This will be presented in ref 1.

We would like to highlight the fact that this preliminary molecular dynamics study of asphaltene nanoaggregation represents a significant advance over many previous asphaltene simulation investigations by the use of (a) long simulation times, allowing us to study the dynamics of asphaltene aggregation and calculate reliable radial distribution functions, (b) the use of explicit solvent molecules in the simulations (it is vital to include their contribution to the binding energy), and (c) the use of optimized molecular structures in line with recent experimental results (mass spectrometry, UV absorption, etc.).

Acknowledgment. The authors thank the Natural Environment Research Council U.K. for funding and Schlumberger Cambridge Research for use of computer resources.

EF800872G